# Supporting Material on: Vibrational spectroscopies in liquid water: On temperature and coordination effects in Raman and infra-red spectroscopies

Rodolphe Vuilleumier
*Processus d'Activation Sélective par Transfert d'Énergie Uni-électronique ou Radiatif (PASTEUR), Département de Chimie, École Normale Supérieure, Paris Sciences et Lettres (PSL) Research University, Sorbonne Université, Centre Nationale de la Recherche Scientifique (CNRS), F-75005 Paris, France*

Ari Paavo Seitsonen
*Institut für Chemie, Universität Zürich, Winterthurerstrasse 190, CH-8057 Zürich and Processus d'Activation Sélective par Transfert d'Énergie Uni-électronique ou Radiatif (PASTEUR), Département de Chimie, École Normale Supérieure, Paris Sciences et Lettres (PSL) Research University, Sorbonne Université, Centre Nationale de la Recherche Scientifique (CNRS), F-75005 Paris, France*

Here we provide further results and background material that further support our investigations and results from the Main Text.

We divide the material in three sections, according to the order found also in the main Manuscript: Structural, dynamical and vibrational properties.

Here we also include some results from simulations that we do not include in the Manuscript, as there is sufficient data from our simulations or we could not afford to evaluate the evaluation of the vibrational spectra, and thus we show some scattered data here.

## I. RESULTS AND DISCUSSIONS

### A. Structural properties

- In Table I we include the average intra-molecular O-H bond lengths and the average dipole moment in the constrained simulations. The same data are found in the Table 2 in the Manuscript, but here we order the entries differently, with $l$ changing on subsequent lines so as to simplify the comparison of the effect of the different value number of accepted hydrogen bonds (HBs) $l$ in the coordination $A_lD_{mn}$. Here we can more clearly see for example that whereas the bond lengths are hardly affected by increasing the $l$ at constant mn, the average dipole moment $\overline{\mu}_W$ clearly increases. Whether this trend would be observed also with the other methods of defining the dipole moment in the condensed phase – here we use the centres of the maximally localised Wannier functions – remains to be investigated in a further study

- In Figure 1 we show the radial distribution functions (RDFs) $g(O-O)$ and $g(O-H)$ and their cumulative integrals. The intra-molecular O-H bond is neglected in the latter quantity

- In Figure 2 we show the $O_c$-O-RDF split between the molecules which are determined to be – solid lines – and not to be – dashed lines – hydrogen bonded in the simulations without a constrained HB coordination

- In Figure 3 we show the RDF of the fifth-nearest neighbour oxygen and hydrogen atoms. These results could eventually be compared to the results obtained for example by Saitta and Datchi [1]

- In Figure 4 we show the $O_c$-O-RDF split between the molecules which are determined to be – solid lines – and not to be – dashed lines – hydrogen bonded in the simulations with a constrained HB coordination on the central molecule $c$

TABLE I. Average intra-molecular bond lengths and dipole moment in the constrained simulations

| $C_{\mathrm{HB}}$ | $d(\mathrm{OH}_a)$ [Å] | $d(\mathrm{OH}_b)$ [Å] | $\overline{\mu}_{\mathrm{W}}$ [D] |
|---|---|---|---|
| $\mathrm{A_0D_{00}}$ | 0.975±0.024 | 0.975±0.024 | 2.06 |
| $\mathrm{A_1D_{00}}$ | 0.976±0.025 | 0.976±0.025 | 2.38 |
| $\mathrm{A_2D_{00}}$ | 0.977±0.024 | 0.977±0.024 | 2.46 |
| $\mathrm{A_0D_{01}}$ | 0.975±0.023 | 0.984±0.024 | 2.23 |
| $\mathrm{A_1D_{01}}$ | 0.975±0.021 | 0.991±0.028 | 2.65 |
| $\mathrm{A_2D_{01}}$ | 0.976±0.024 | 0.997±0.028 | 2.80 |
| $\mathrm{A_0D_{11}}$ | 0.981±0.026 | 0.981±0.025 | 2.29 |
| $\mathrm{A_1D_{11}}$ | 0.986±0.028 | 0.986±0.028 | 2.78 |
| $\mathrm{A_2D_{11}}$ | 0.992±0.028 | 0.992±0.028 | 3.07 |
| $\mathrm{A_2D_{11}S}$ | 0.997±0.029 | 0.997±0.029 | 3.20 |
| $\mathrm{A_3D_{11}}$ | 0.995±0.030 | 0.993±0.027 | 2.97 |
| $\mathrm{A_3D}_{nm}$ | 0.991±0.029 | 0.991±0.027 | 2.97 |

- In Figure 5 we show the cumulative integrals of the radial distribution functions in the systems where the HB coordination was fixed during the simulation; $\mathrm{O_{ctr}}$-O, $\mathrm{O_{ctr}}$-H, $\mathrm{H_{ctr}}$-O, where the sub-script "ctr" refers to the central, constrained molecule. These graphs only acts as a verification that indeed the restraint on the coordination of the HBs has been effective in the simulations

- In Figure 6 we show the distribution of HB configurations $C_{\mathrm{HB}}$ in the trajectories in which the coordination of a molecule has been constrained. This is used only to verify that the constraint indeed yields the targeted HB coordination. There are some deviations, which are probably due to the different form and parametres of the function $C_{\mathrm{L_1,L_2}}$, being purely radial, used in the confinement of the coordination and the definition of a HB, that also includes a requirement on the angle $\mathrm{H{-}O\cdots O}$

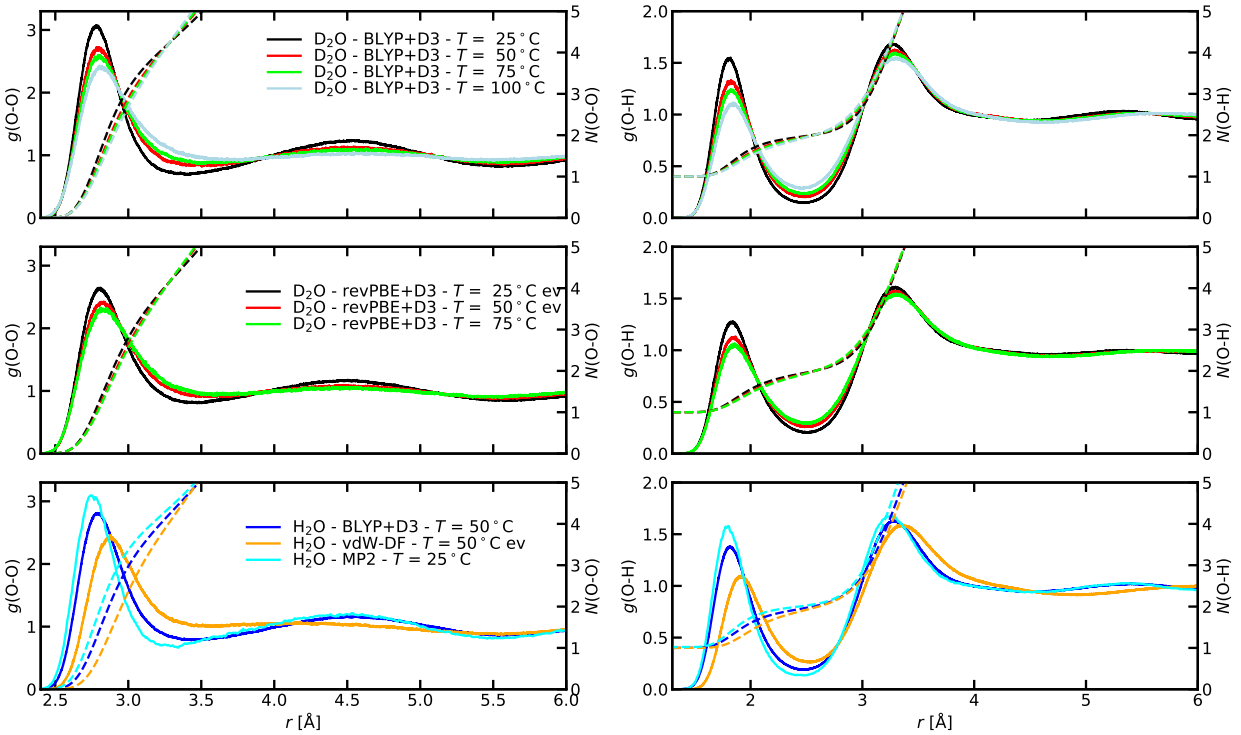


FIG. 1. Radial distribution functions – solid lines, left-side vertical axis – and their cumulative integrals – dashed line, right-size vertical axis. The closest intra-molecular O-H bond is neglected

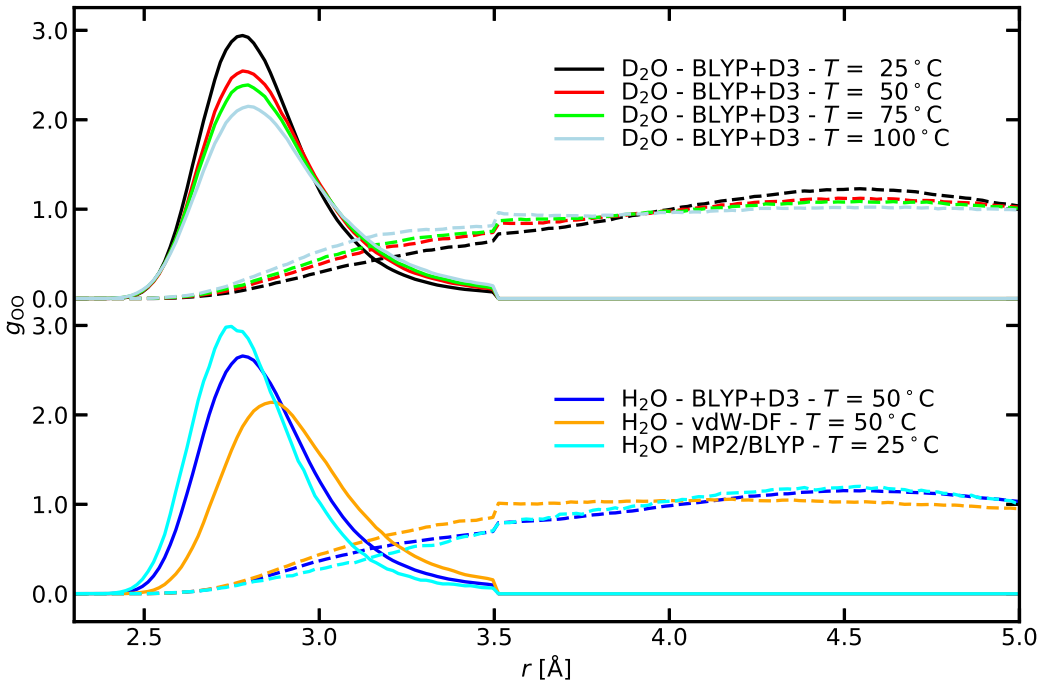


FIG. 2. $O_c$-O-RDF split between hydrogen bonded and pair of molecules in simulations without a constraint on the central molecule $c$; solid lines: HB, dashed lines: no HB

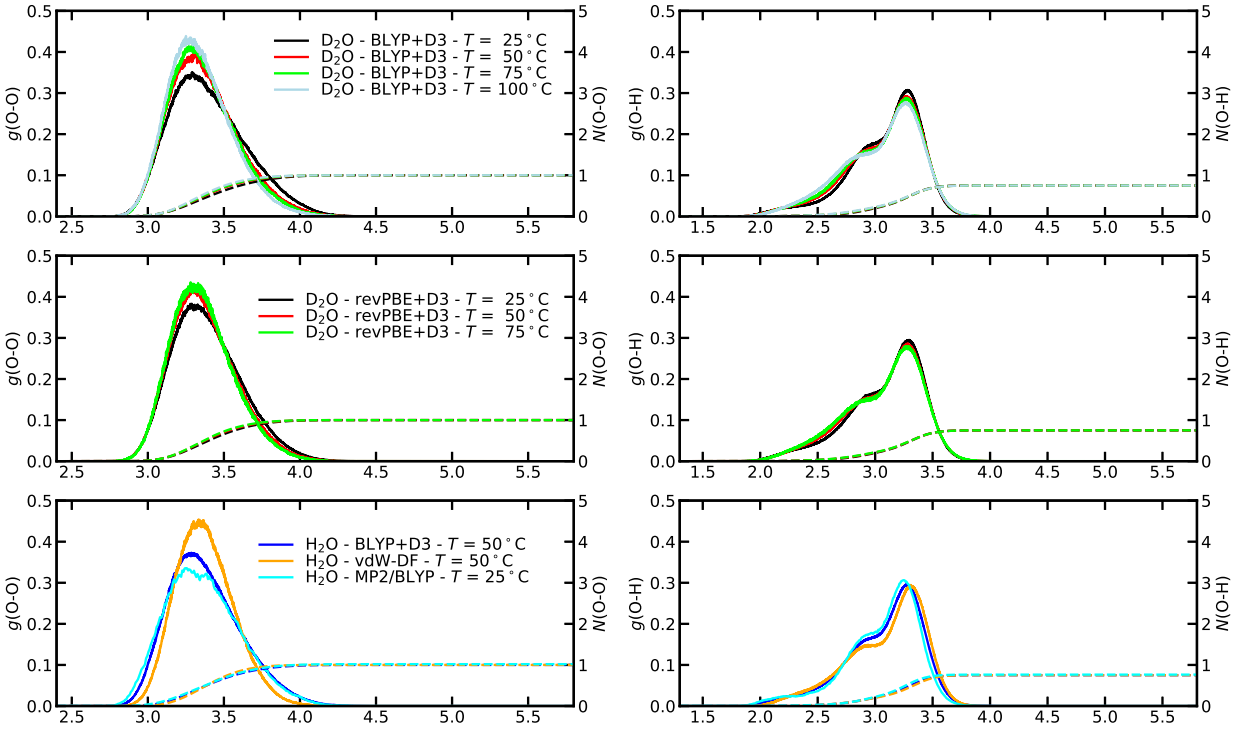


FIG. 3. RDF of the fifth-nearest neighbour oxygen – left Panels – and hydrogen – right Panels – from the central oxygen atom

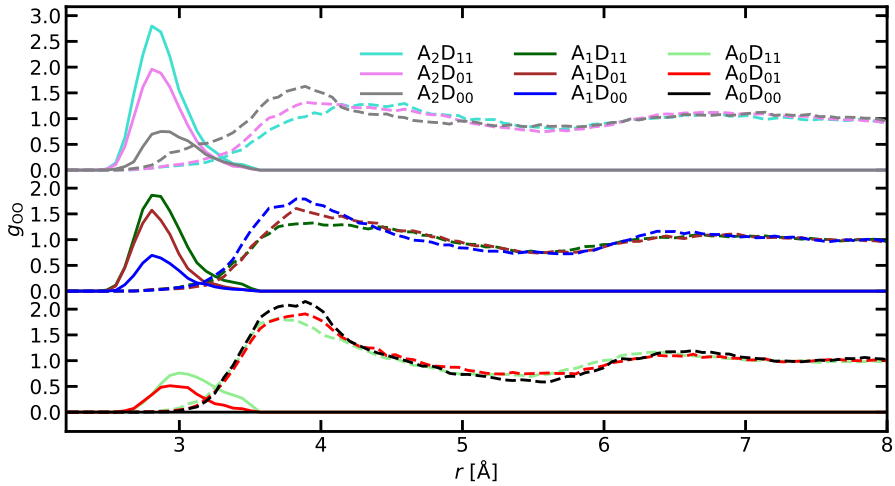


FIG. 4. $O_c$-O-RDF split between molecules which are determined to be – solid lines – and not to be – dashed lines – hydrogen bonded in simulations with constrained HB coordination on the central molecule $c$; solid lines: HB, dashed lines: no HB

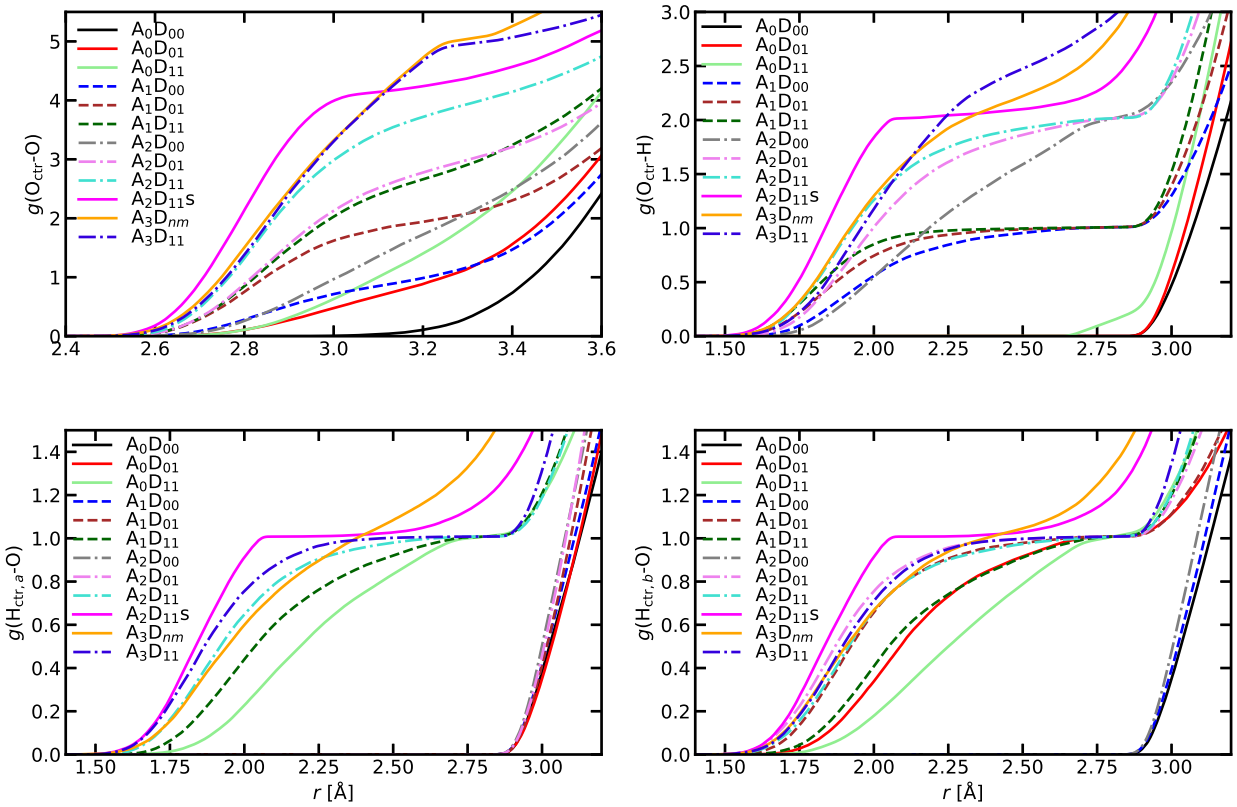


FIG. 5. Cumulative integrals of the radial distribution functions in the simulations where the HB coordination was constrained; $O_{ctr}$-O, $O_{ctr}$-H, $H_{ctr}$-O, where the sub-script "ctr" refers to the central, constrained molecule

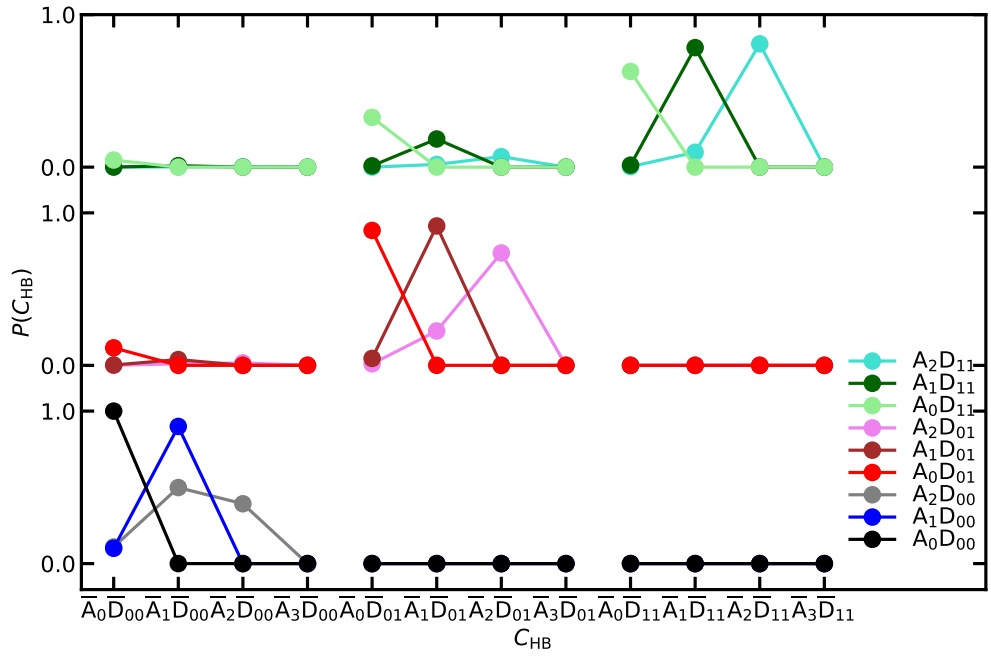


FIG. 6. Distribution of HB configurations $C_{HB}$ in the trajectories in which the coordination of a molecule has been constrained

## B. Dynamical properties

- In Figure 7 we show the diffusion constant $D$ of $D_2O$ as a function of temperature from the experiments [2] and the present simulations; Expr* is the experimental data minus the finite-size correction [3, 4]

$$D_{\mathrm{PBC}}(L) = D - \frac{k_{\mathrm{B}} T \zeta}{6\pi\eta L} \ ,$$

where $D_{\mathrm{PBC}}(L)$ is the value obtained from simulation in a periodic cell of length $L$, $\zeta = 2.837$ is a numerical coefficient and $\eta$ is the dynamic viscosity; as the latter is not known from the simulations without further, tedious simulations it is common to indeed extract the value the real liquid, from experiments, ought to have if it was periodic in the same cell as in the actual simulations.

We find that the values of $D$ with the BLYP+D3 approximation are generally too low, whereas with the revPBE+D3 the water is more diffusive, in particular at the low temperatures around the room temperature, where the BLYP+D3 is known to be rather an amorphous liquid, due to too low diffusivity and too low a melting temperature

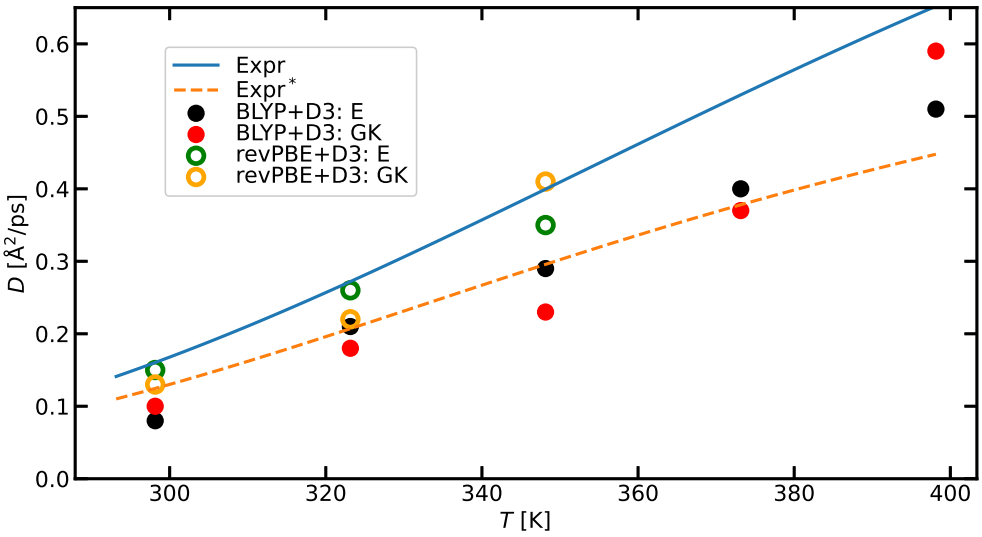


FIG. 7. Diffusion constant of $D_2O$ as a function of temperature from the experiments [2] and the present simulations; Expr* is the experimental data minus the finite-size correction

- In Figure 8 we show the computed static di-electric constant $\varepsilon$ as a function of time. As is known in the literature [5] this value converges only very slowly with the length of the simulation time; therefore we only cite the values that we obtain very carefully, as it can also be seen that the value is most likely not yet settled even roughly during our simulations

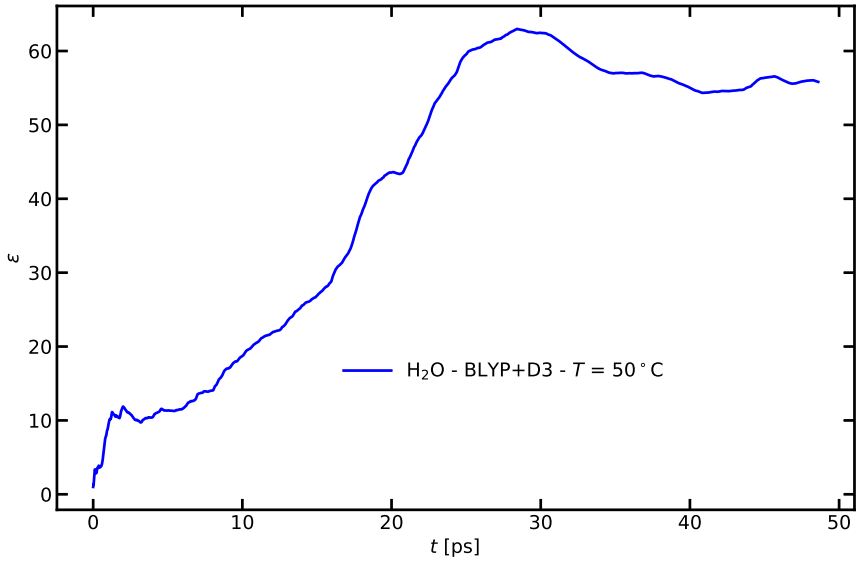


FIG. 8. The value of the static di-electric constant $\varepsilon$ at as a function of the simulation time

- In Figures 9 and 10 we show the rotational correlation of the water molecules in the simulations, and in Figure 11 the cumulative integral of it.

  These quantities give insight into the rotational dynamics of the water molecules. We see basically the same trend as in the diffusivity, for example, as the rotational correlation attains a shorter duration as the temperature is increased in the simulation. Also the use of the approximation revPBE+D3 leads to faster loss of rotational history than the BLYP+D3 at the corresponding temperature. We see also that the simulations without the inclusion of the van der Waals term, either with a specific density functional or at least with a semi-empirical treatment, leads to very slow relaxational dynamics. Also the rotational dynamics from the MP2 simulations is quite slow; the trajectory [6] is too slow to reach convergence in the integrated value, but the initial slope is clearly less steep than the simulation with the revPBE+D3 at the $T = +25°$C for example

- In Figure 12 we show the rotational lifetimes $\tau_1$, $\tau_2$ and $\tau_{12}$ as in Ref [7]. The non-monotonic appearance of the values with the increasing temperature probably renders the limited statistics contained in our simulations.

  These quantities give further insight into the rotational dynamics of the water molecules as the rotational correlation above. We obtain similar numerical values as in that previous study, although there the classical force field TIP5P was used. We see clear decreasing lifetimes upon increasing the temperatures, and the liftimes are shorter with the revPBE+D3 than the BLYP+D3 approach. This correlates again well with the other observables that we have evaluated that indicate the revPBE+D3 to yield more liquid-like, diffusive and rotating water molecules already at the lowest simulated temperature

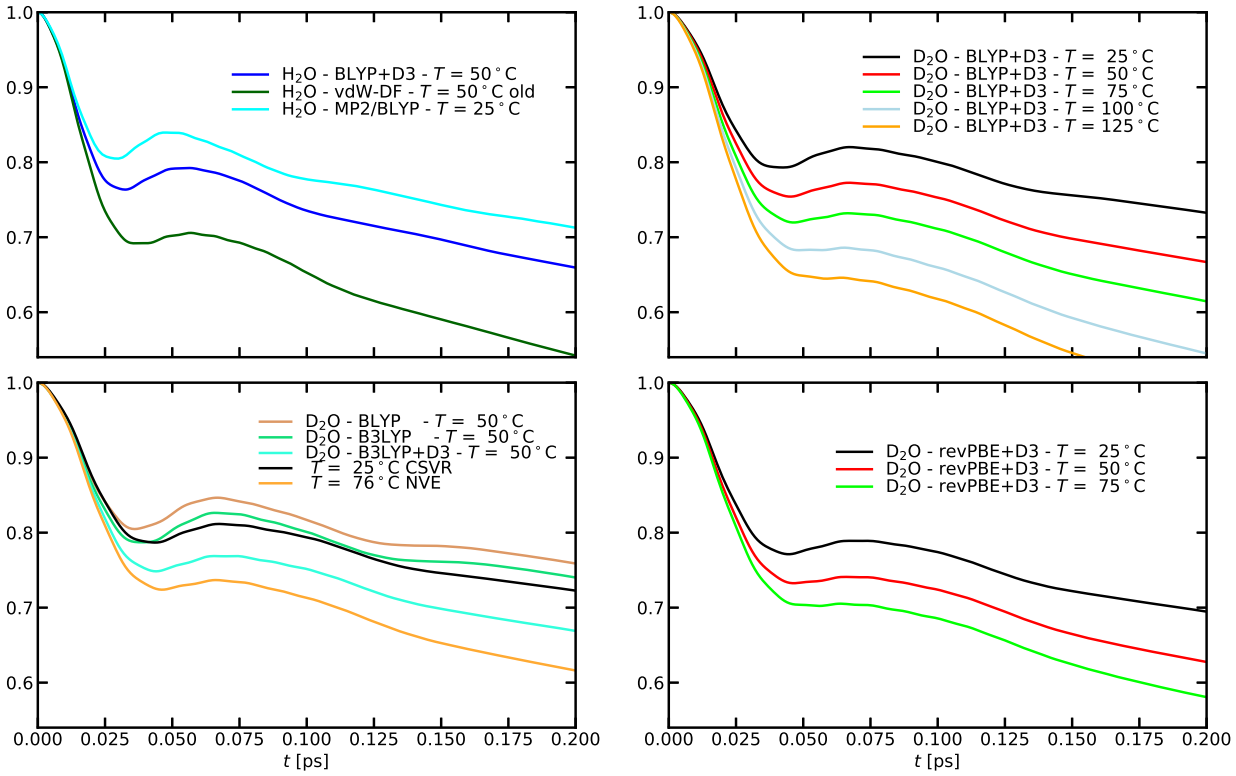


FIG. 9. The initial rotational correlation of the water molecules in the simulations

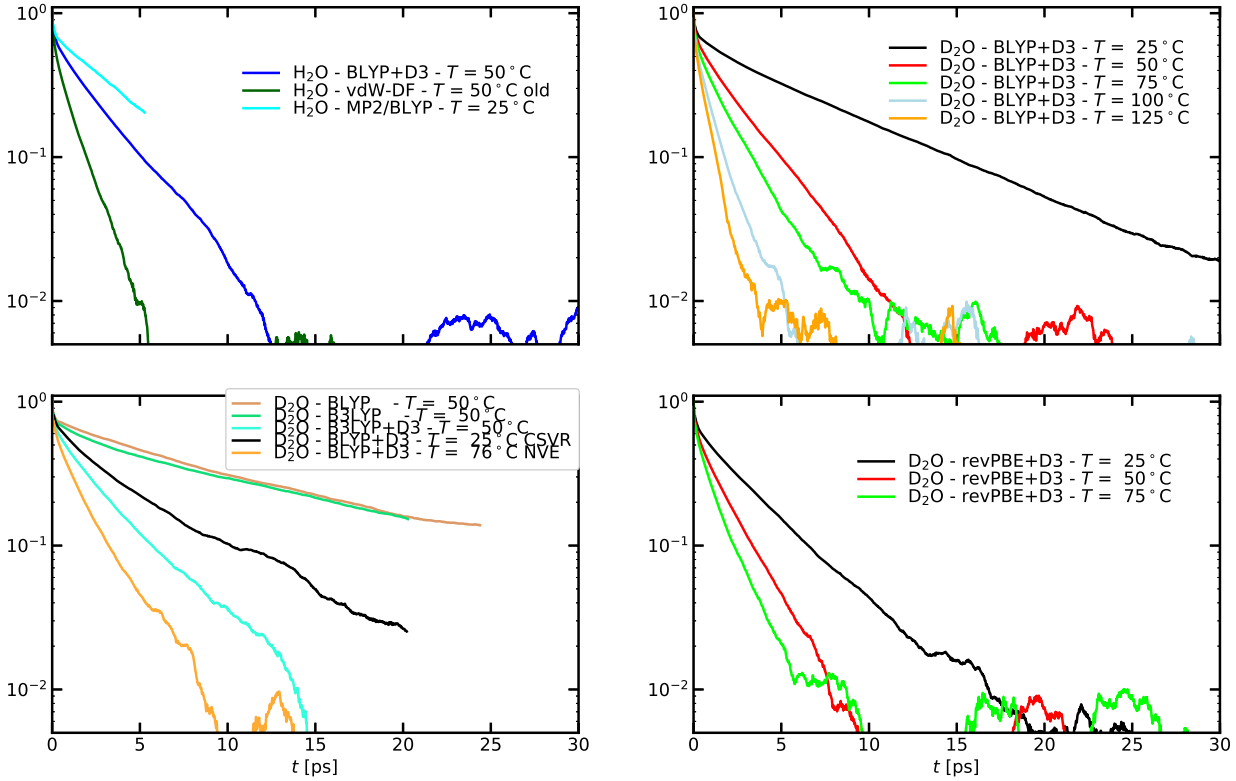


FIG. 10. The relaxation of the rotational correlation of the water molecules in the simulations

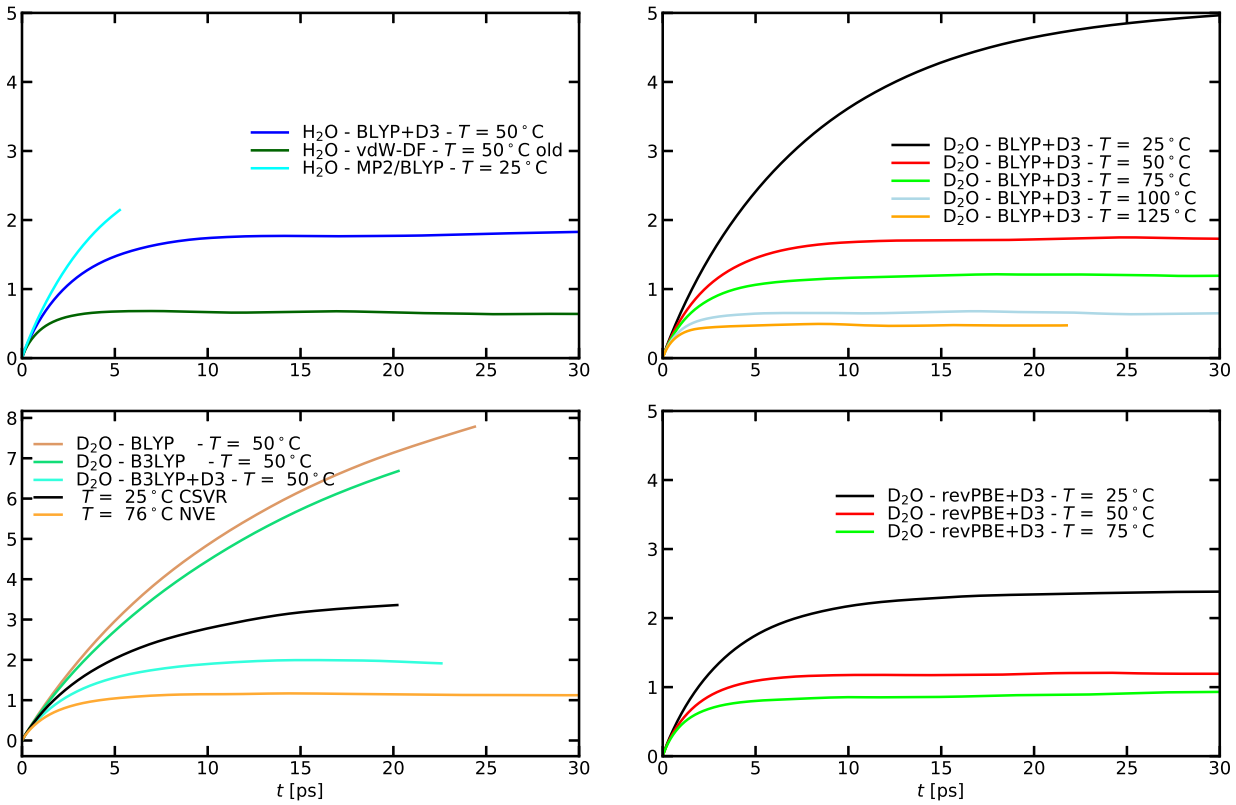


FIG. 11. The cumulative rotational correlation of the water molecules in the simulations

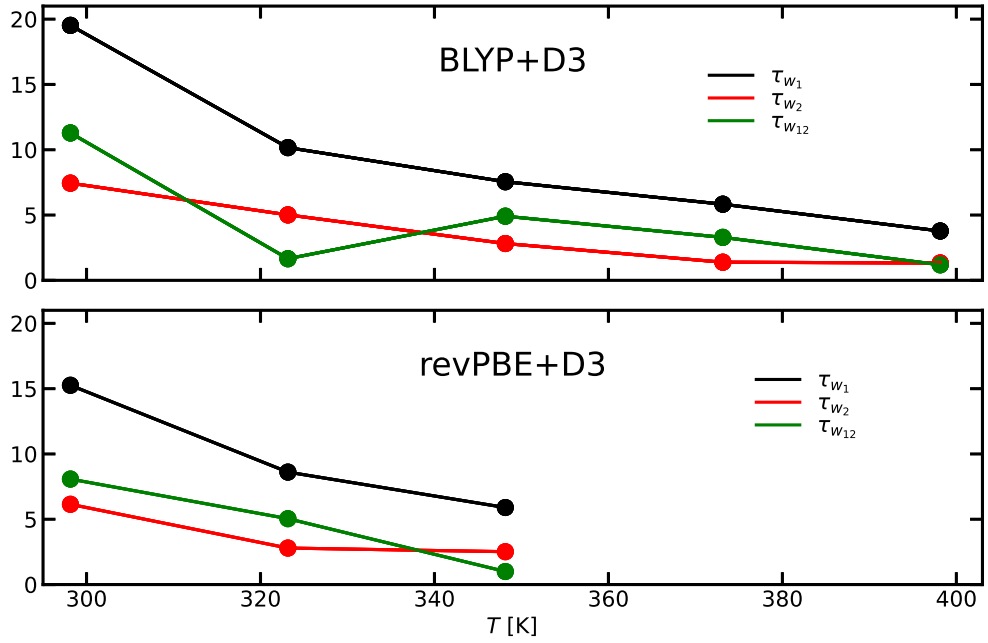


FIG. 12. The rotational lifetimes $\tau_1$, $\tau_2$ and $\tau_{12}$ used to characterise the hydrogen bond lifetimes

### C. Vibrational properties

- In Figures 13 and 14 we show the power spectrum of H/D and O, respectively, in the simulated systems. The magnitude is normalised at the maximum. MP2 frequency scale has been multiplied by a constant 0.94

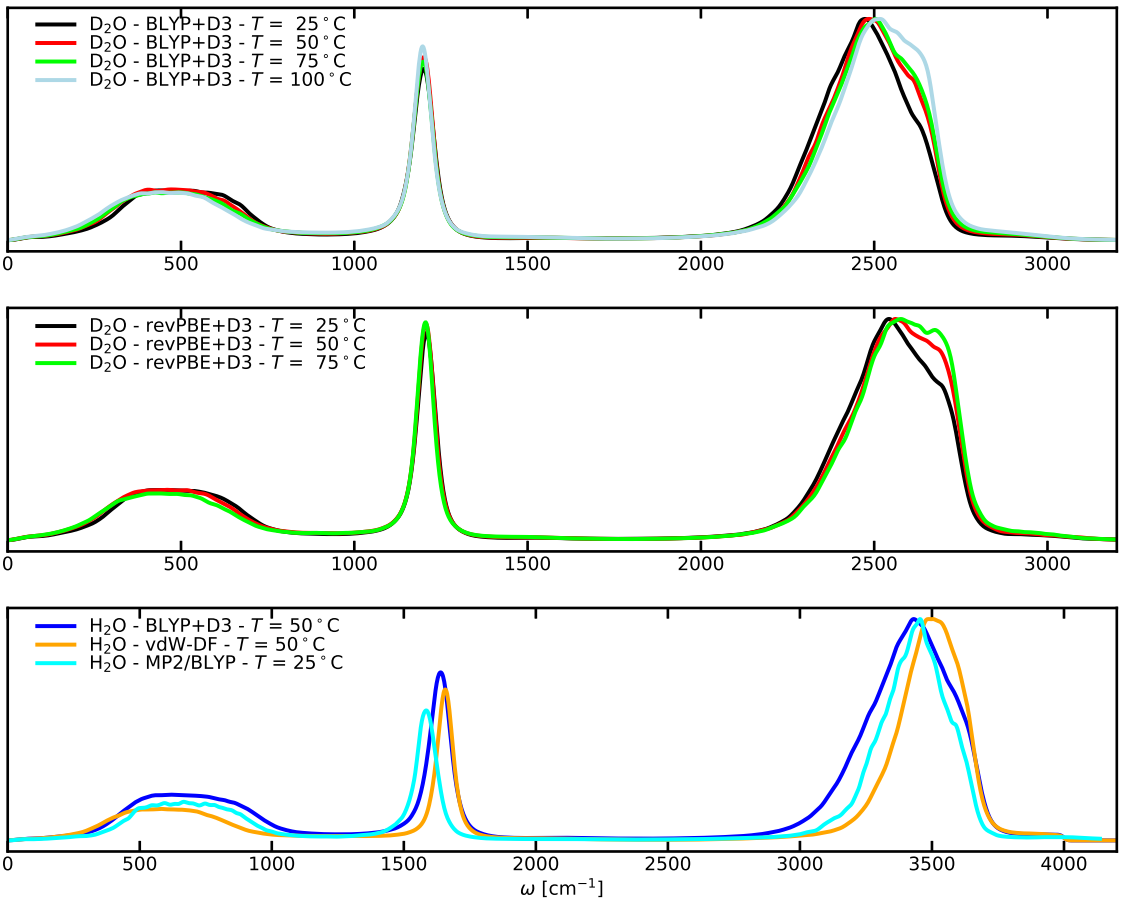


FIG. 13. Power spectrum of H/D in the simulated systems. The magnitude is normalised at the maximum. MP2 frequency scale has been multiplied by a constant

- In Figure 15 we show the power spectrum of the central oxygen atom in the isotopic mixtures

- In Figure 16 we show the infra-red spectra in $D_2O$ – left Panel – and $H_2O$ – right Panel – with the experimental data from Ref [8]

- In Figure 17 we show the power spectra of intra-molecular bond lengths of a water molecule in $D_2O$ in restricted HB coordinations $C_{\rm nm}$; left, $d(\mathrm{OH_a})$ – solid line –, $d(\mathrm{OH_b})$ – dashed line –, right $d$(symm) – solid line –, $d$(asymm) – dashed line

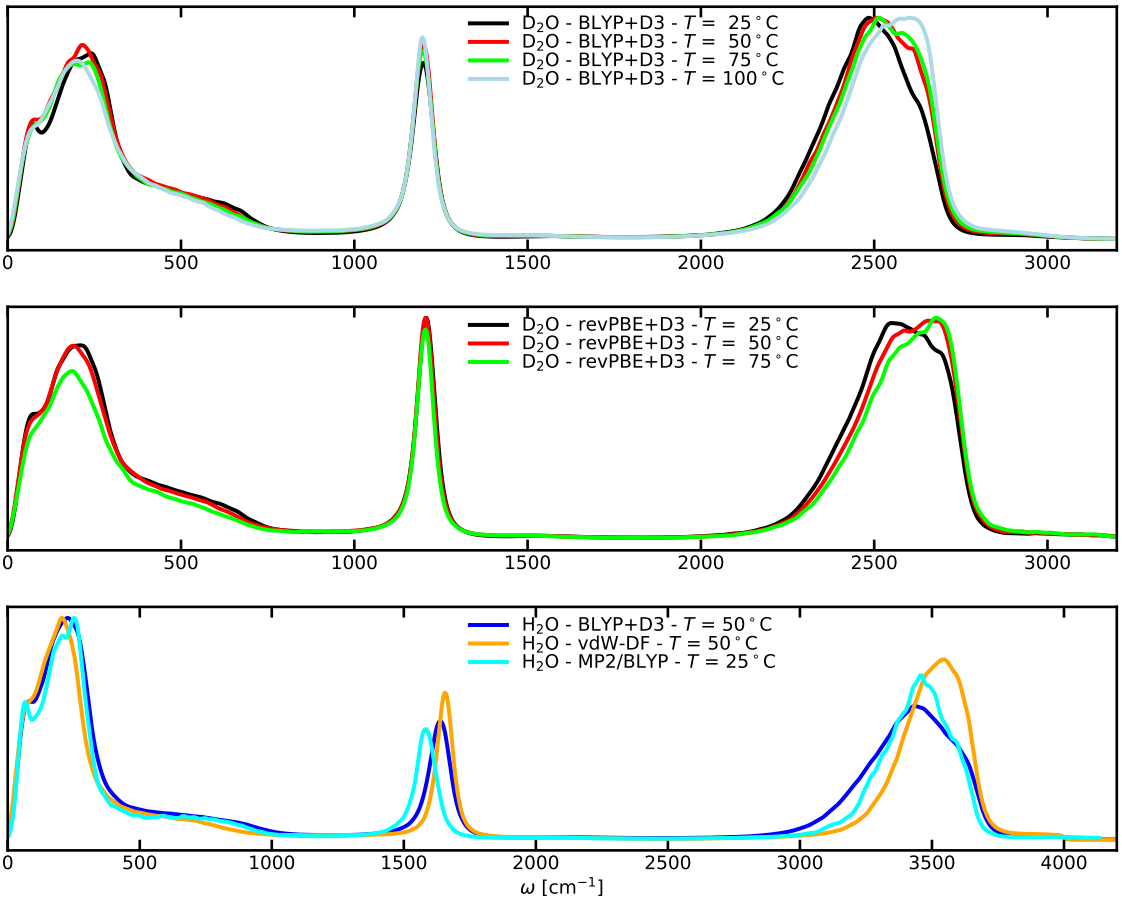


FIG. 14. Power spectrum of O in the simulated systems

- In Table II we show the frequencies obtained from localised ENMA vibrations at different constrained coordinations $C_{\rm nm}$ on the central water molecule

- In Figure 18 we show the power spectra on the deuterium atoms – top panel – and the localised power spectra from ENMA – bottom panel – in the simulations with the restrained coordination of the hydrogen bonds

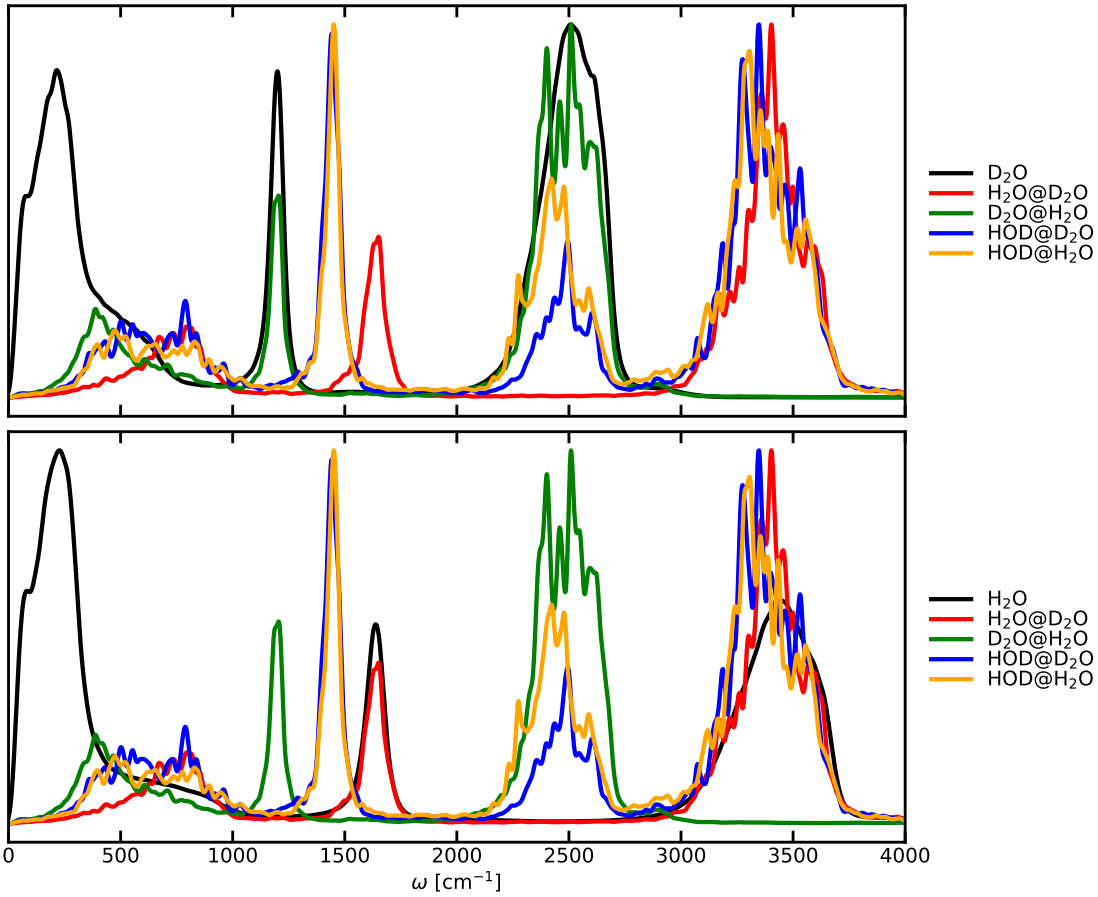


FIG. 15. Power spectrum of the central oxygen atom in the isotopic mixtures

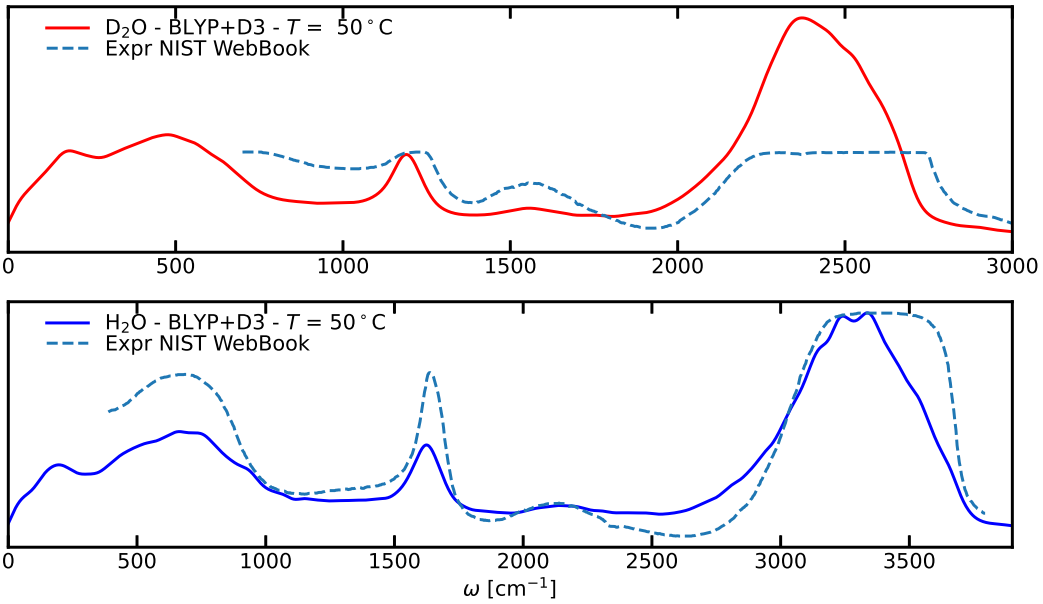


FIG. 16. Infra-red spectra in $D_2O$ – left Panel – and $H_2O$ – right Panel – with the experimental data [8]

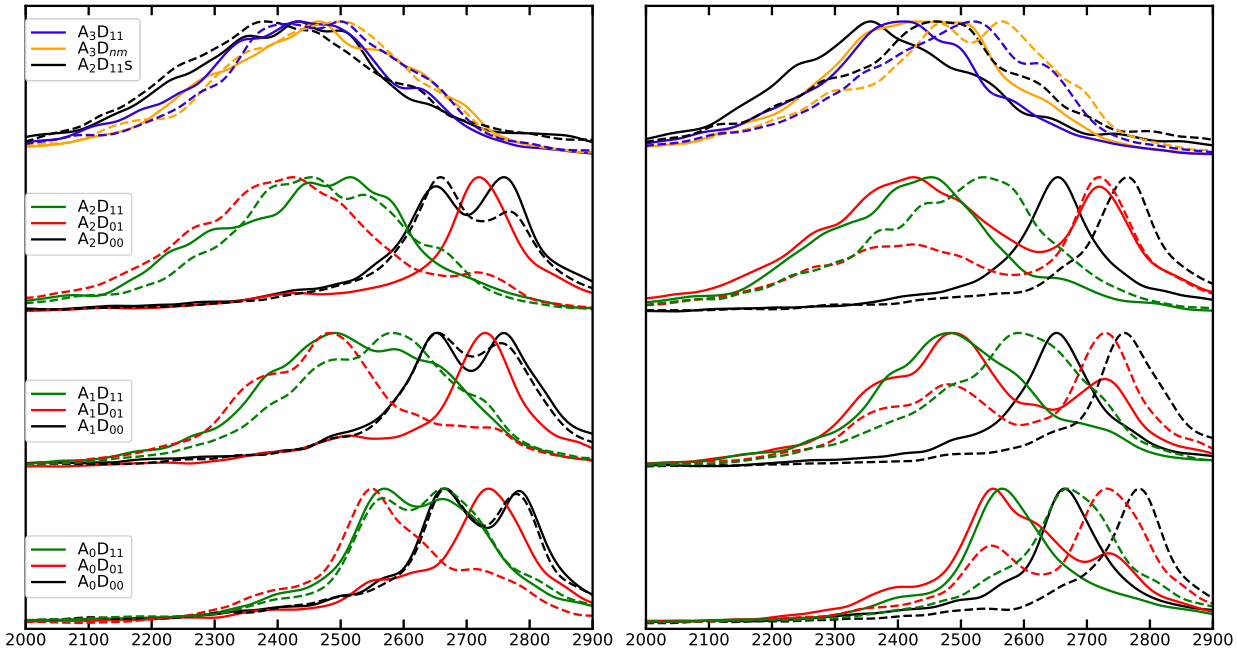


FIG. 17. Power spectra of intra-molecular bond lengths of a water molecule in $D_2O$ in restricted coordinations; left, $d(OH_a)$ (straight line), $d(OH_b)$ (dashed), right $d$(symm) (straight), $d$(asymm) (dashed)

TABLE II. Frequencies obtained from localised ENMA vibrations at different coordinations $n$ on the central water molecule

| $C_{HB}$ | $\omega$ | | | $\Delta\omega$ | | |
|---|---|---|---|---|---|---|
| $A_0D_{00}$ | 1234 | 2686 | 2797 | ref | ref | ref |
| $A_1D_{00}$ | 1242 | 2678 | 2793 | 9 | -8 | -4 |
| $A_2D_{00}$ | 1260 | 2678 | 2788 | 26 | -8 | -9 |
| $A_0D_{01}$ | 1224 | 2587 | 2756 | -10 | -99 | -41 |
| $A_1D_{01}$ | 1233 | 2500 | 2750 | -1 | -186 | -47 |
| $A_2D_{01}$ | 1246 | 2428 | 2744 | 12 | -258 | -52 |
| $A_0D_{11}$ | 1240 | 2628 | 2722 | 6 | -58 | -74 |
| $A_1D_{11}$ | 1230 | 2531 | 2628 | -4 | -155 | -168 |
| $A_2D_{11}$ | 1226 | 2449 | 2529 | -8 | -237 | -268 |
| $A_2D_{11}s$ | 1224 | 2431 | 2498 | -10 | -255 | -298 |
| $A_3D_{11}$ | 1204 | 2453 | 2529 | -30 | -233 | -268 |
| $A_3D_{nm}$ | 1204 | 2453 | 2529 | -30 | -233 | -268 |

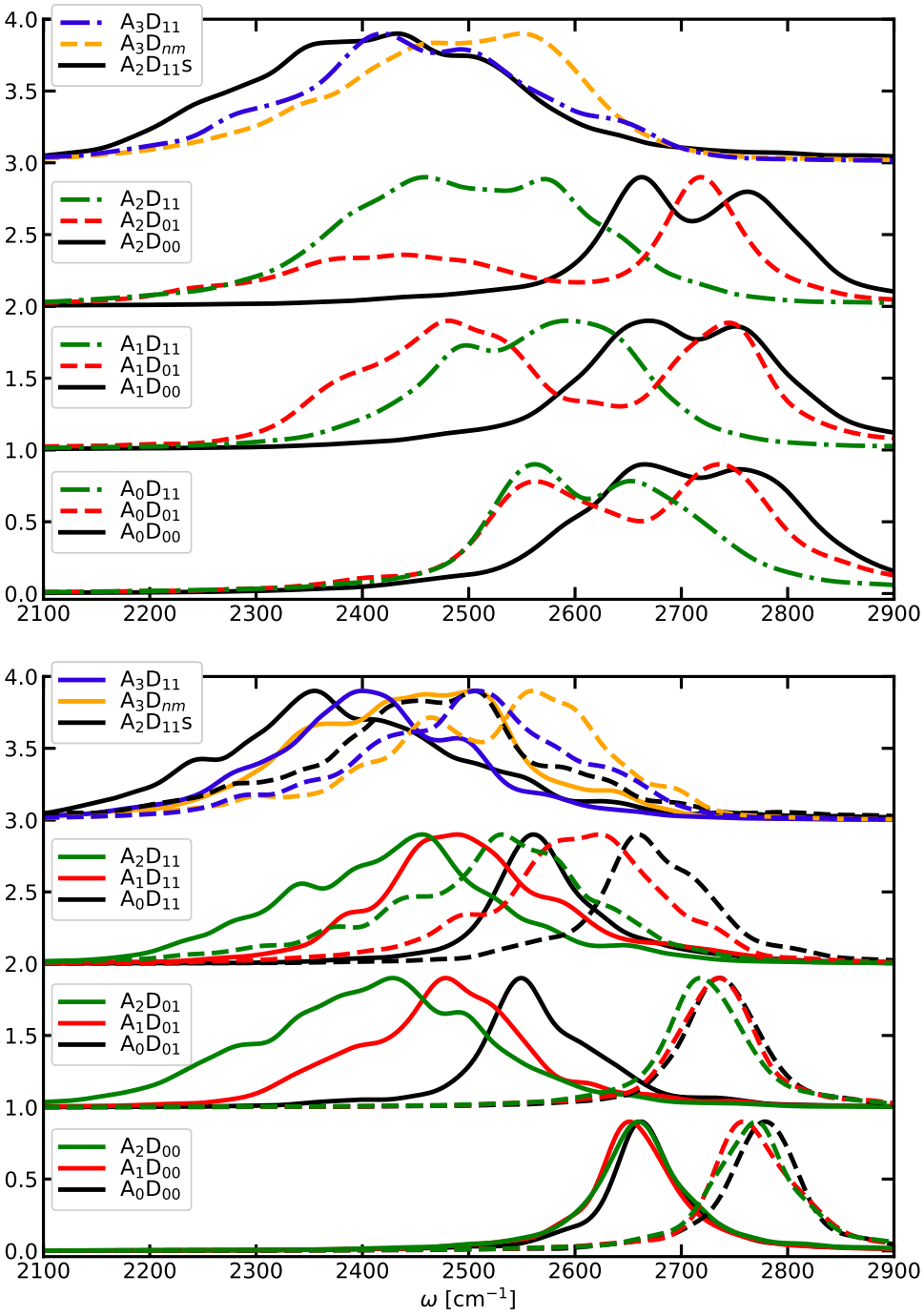


FIG. 18. The power spectra of the deuterium atoms – top panel – and the localised power spectra from ENMA – bottom panel – in the simulations with the restrained coordination of the hydrogen bonds

[1] A. M. Saitta and F. Datchi, Structure and phase diagram of high-density water: The role of interstitial molecules, Physical Review E **67**, 020201 (2003).

[2] P. Han and D. M. Bartels, Journal of Physical Chemistry **100**, 5597 (1996), experimental results on the diffusion constant.

[3] B. Dünweg and K. Kremer, Molecular dynamics simulation of a polymer chain in solution, Journal of Chemical Physics **99**, 6983 (1993), finite-size correction on diffusion.

[4] T. D. Kühne, M. Krack, and M. Parrinello, Static and dynamical properties of liquid water from first principles by a novel Car-Parrinello-like approach, Journal of Chemical Physics **99**, 6983 (2009).

[5] C. Zhang, J. Hutter, and M. Sprik, Computing the Kirkwood g-factor by combining constant Maxwell electric field and electric displacement simulations: Application to the dielectric constant of liquid water, Journal of Physics Chemical Letters **7**, 2696 (2016).

[6] M. D. Ben, J. Hutter, and J. VandeVondele, Raman spectra from ab initio molecular dynamics and its application to liquid s-methyloxirane, J. Chem. Phys. **143**, 054506 (2015).

[7] P. Raiteri, A. Laio, and M. Parrinello, Correlations among hydrogen bonds in liquid water, Physics Review Letters **93**, 087801 (2004).

[8] P. J. Linstrom and W. G. Mallard, eds., *NIST Chemistry WebBook, NIST Standard Reference Database Number 69* (National Institute of Standards and Technology, 2023).